

Electronic Supplementary Information

Pearson's principle-inspired strategy for the synthesis of amorphous transition metal hydroxide hollow nanocubes for electrocatalytic oxygen evolution

Linlin Yang,^a Bin Zhang,^{*a} Wenjie Ma,^a Yunchen Du,^a Xijiang Han^a and Ping Xu^{*a}

^a. MIIT Key Laboratory of Critical Materials Technology for New Energy Conversion and Storage, School of Chemistry and Chemical Engineering, Harbin Institute of Technology, Harbin 150001, China. Email: pxu@hit.edu.cn (P.X.); zhangbin_hit@aliyun.com (B.Z.)

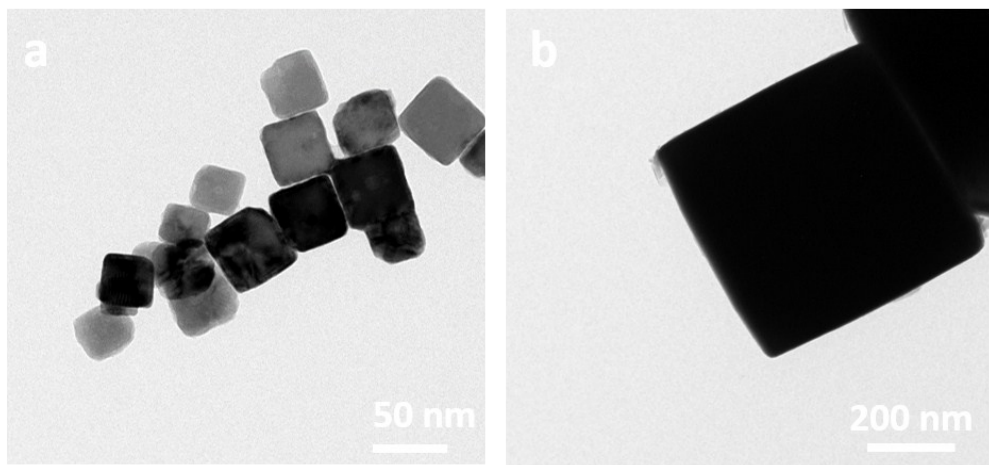


Fig. S1. TEM images of the as-prepared (a) 50 nm Cu₂O templates (b) 500 nm Cu₂O templates.

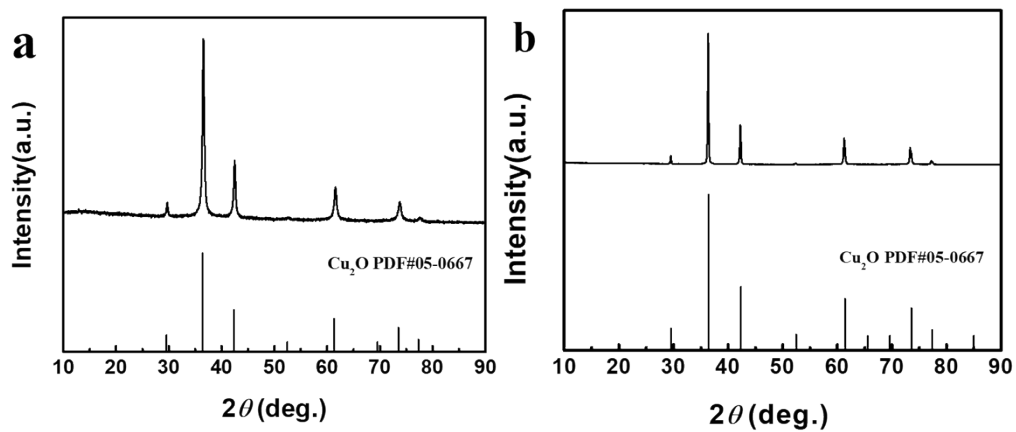


Fig. S2. XRD patterns of the as-prepared (a) 50 nm Cu₂O templates (b) 500 nm Cu₂O templates.

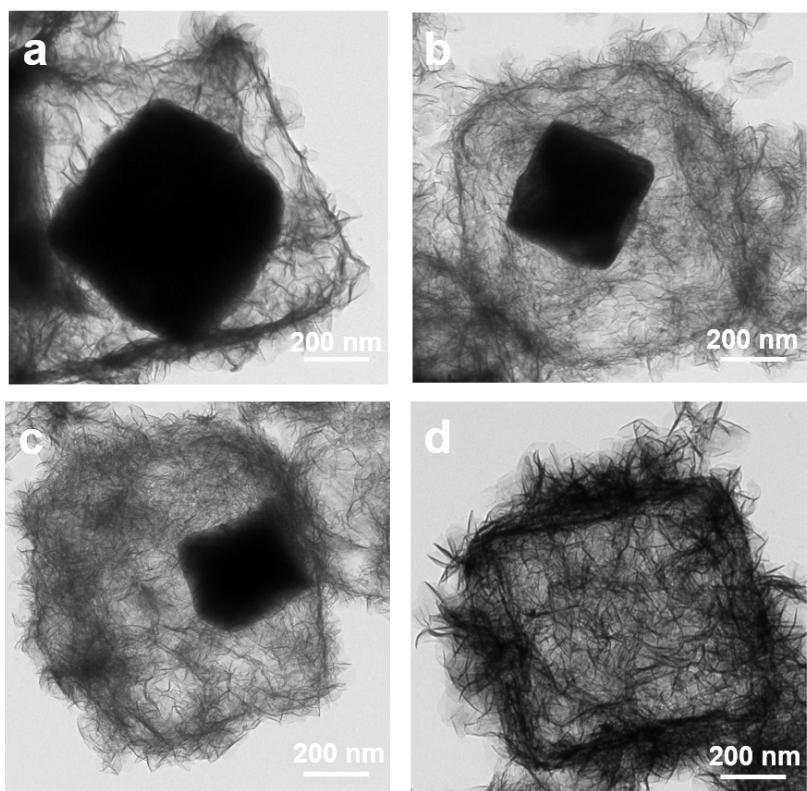


Fig. S3. TEM images of intermediates of $\text{Co}(\text{OH})_2$ at different reaction time: (a) 1 min, (b) 2 min, (c) 5 min, and (d) 10 min.

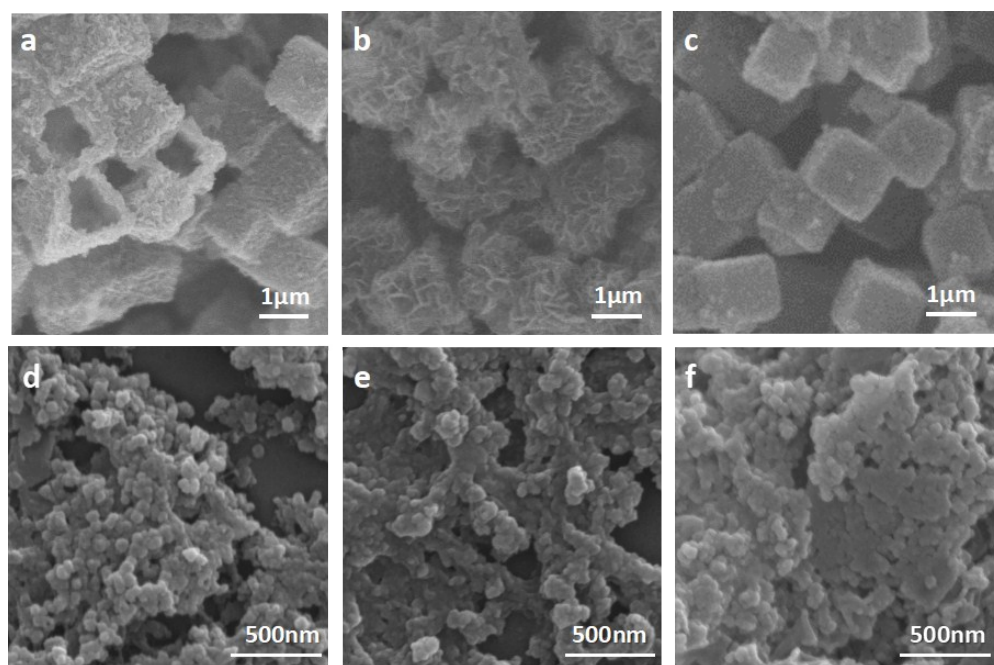


Fig. S4. SEM images of (a) $\text{Fe}(\text{OH})_3$ (500 nm), (b) $\text{Co}(\text{OH})_2$ (500 nm), (c) $\text{Ni}(\text{OH})_2$ (500 nm), (d) $\text{Fe}(\text{OH})_3$ (50 nm), (e) $\text{Co}(\text{OH})_2$ (50 nm), and (f) $\text{Ni}(\text{OH})_2$ (50 nm) hollow nanocubes.

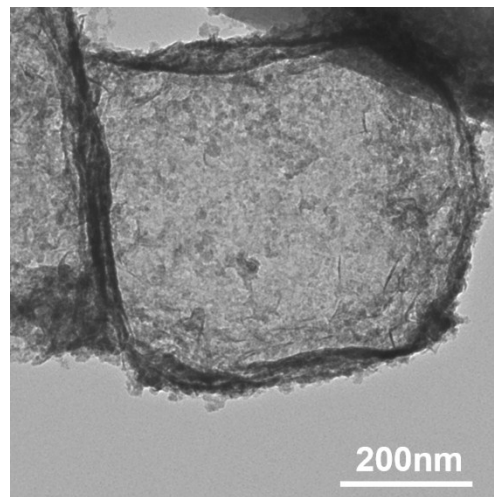


Fig. S5. TEM images of the as-prepared $\text{Fe}(\text{OH})_3$ (500 nm) hollow nanocubes by using $\text{FeCl}_3 \cdot 6\text{H}_2\text{O}$.

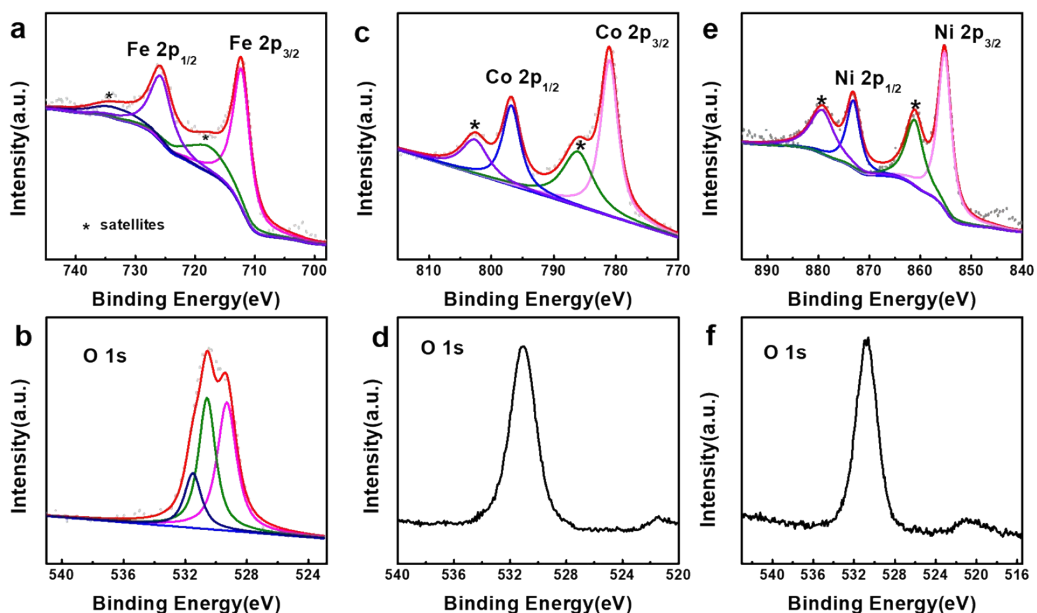


Fig. S6. XPS spectra of the as-prepared (a, b) iron hydroxide (500 nm), (c, d) cobalt hydroxide (500 nm), and (e, f) nickel hydroxide (500 nm).

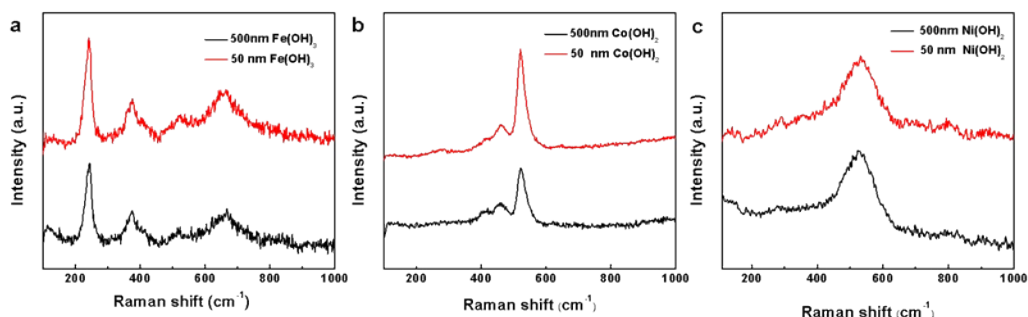


Fig. S7. Raman spectra of (a) $\text{Fe}(\text{OH})_3$ (500 nm) and $\text{Fe}(\text{OH})_3$ (50 nm), (b) $\text{Co}(\text{OH})_2$ (500 nm) and $\text{Co}(\text{OH})_2$ (50 nm), and (c) $\text{Ni}(\text{OH})_2$ (500 nm) and $\text{Ni}(\text{OH})_2$ (50 nm).

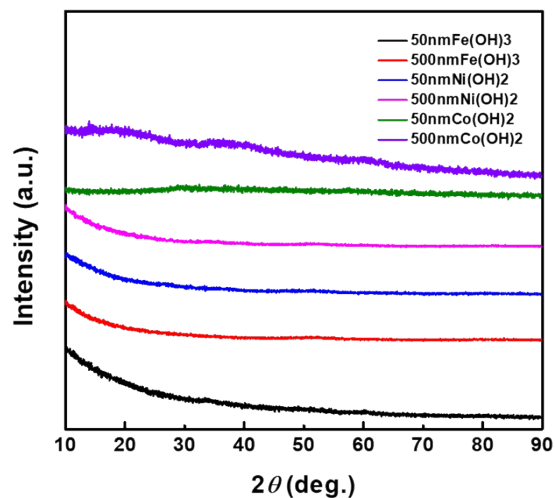


Fig. S8. XRD patterns of Fe(OH)₃ (500 nm), Co(OH)₂ (500 nm), Ni(OH)₂ (500 nm), Fe(OH)₃ (50 nm), Co(OH)₂ (50 nm), and Ni(OH)₂ (50 nm).

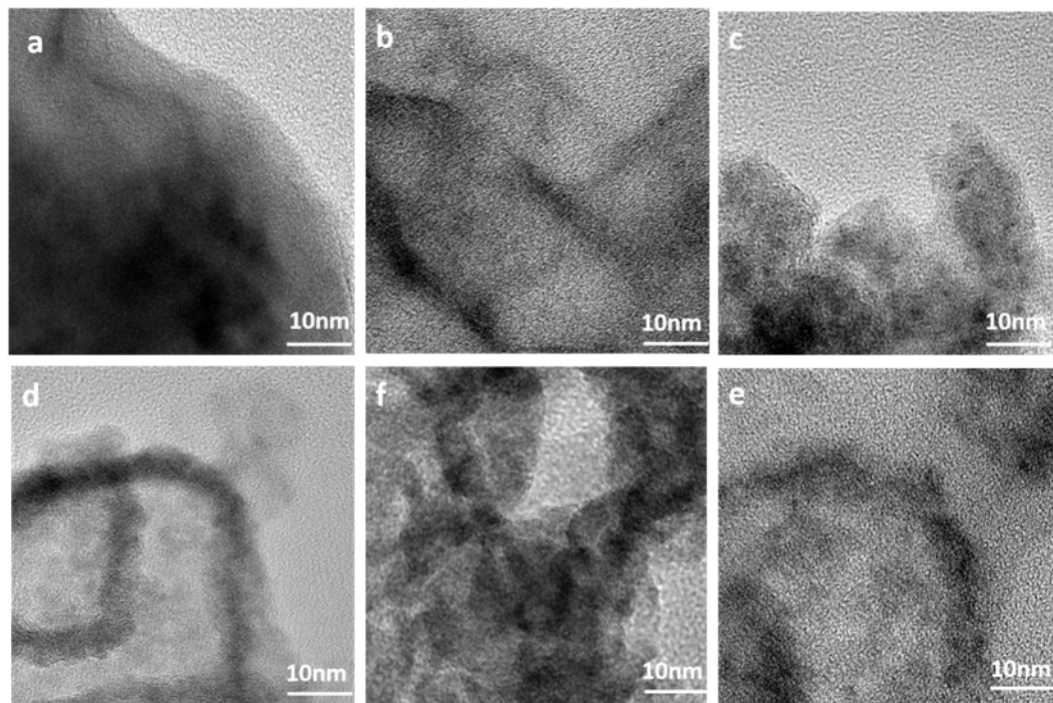


Fig. S9. HR-TEM images of (a) Fe(OH)₃ (500 nm), (b) Co(OH)₂ (500 nm), (c) Ni(OH)₂ (500 nm), (d) Fe(OH)₃ (50 nm), (e) Co(OH)₂ (50 nm), and (f) Ni(OH)₂ (50 nm) hollow nanocubes.

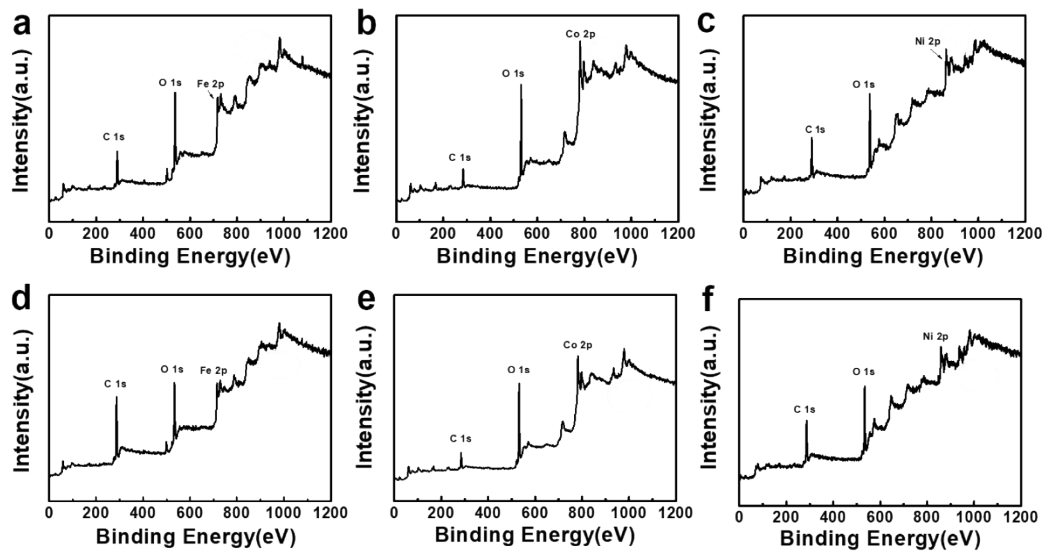


Fig. S10. The full range XPS survey spectra of the as-prepared (a) Fe(OH)_3 (500 nm), (b) Co(OH)_2 (500 nm), (c) Ni(OH)_2 (500 nm), (d) Fe(OH)_3 (50 nm), (e) Co(OH)_2 (50 nm), (f) Ni(OH)_2 (50 nm) hollow nanocubes.

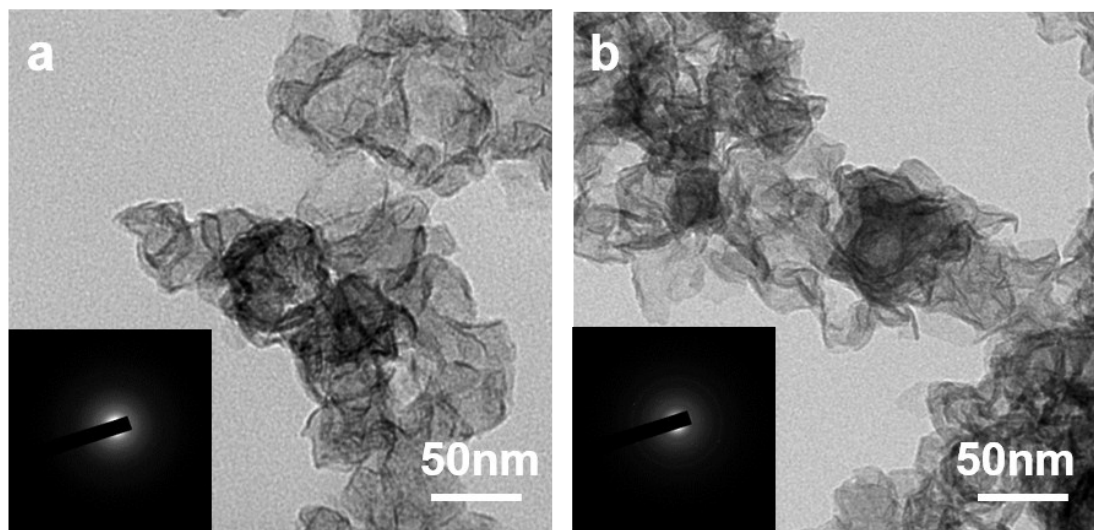


Fig. S11. TEM and SAED images of the as-prepared (a) Mn(OH)_2 (50 nm), (b) Zn(OH)_2 (50 nm) hollow nanocubes.

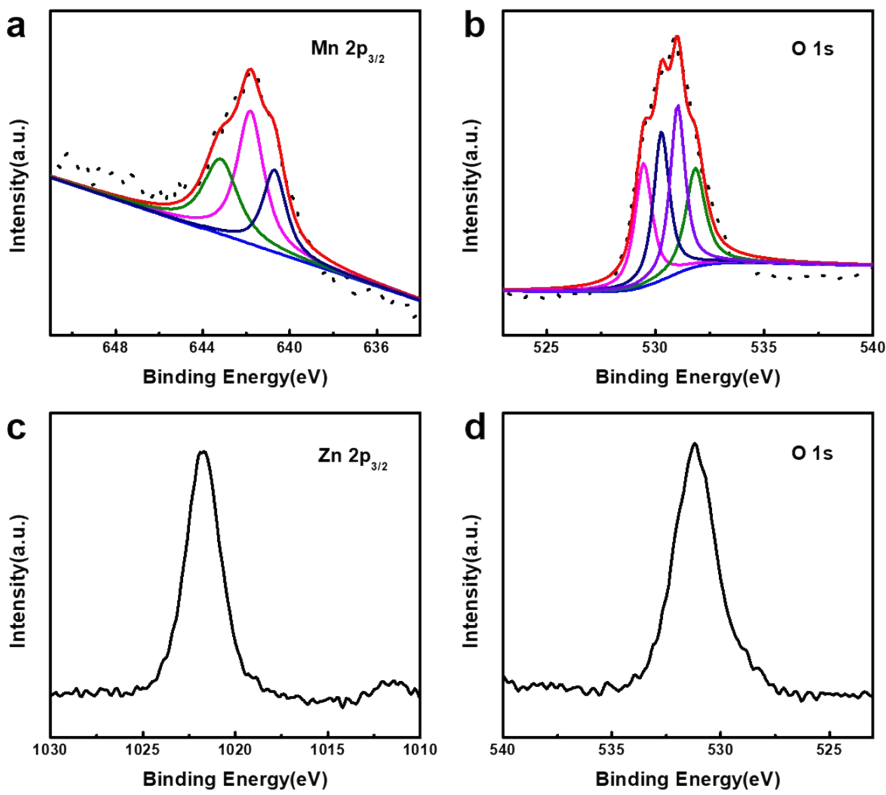


Fig. S12. XPS spectra of the as-prepared samples. (a) Mn 2p and (b) O 1s of manganese hydroxide (50 nm), (c) Zn 2p and (d) O 1s of zinc hydroxide (50 nm).

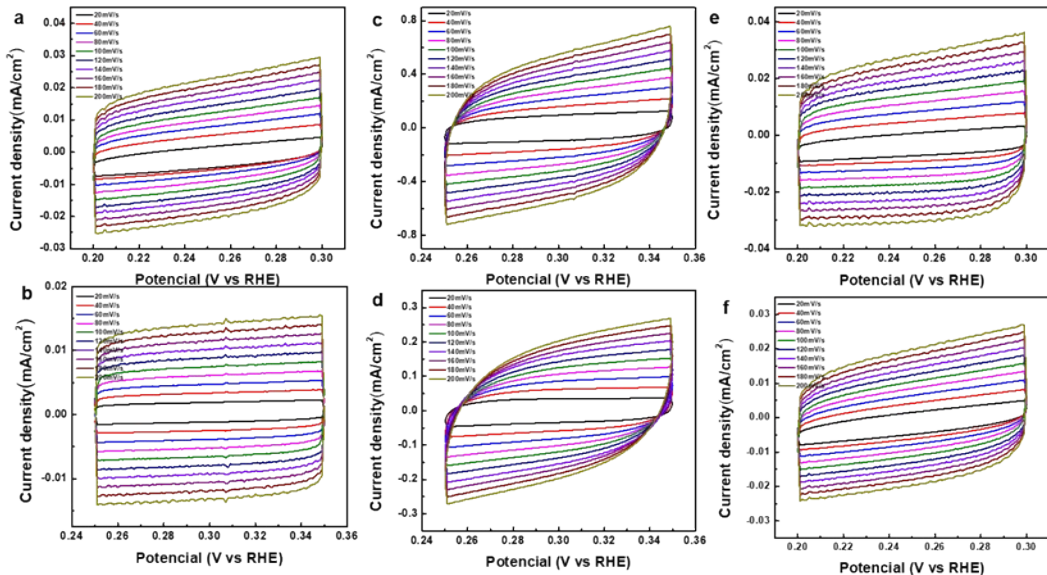


Fig. S13. Cyclic voltammetry curves of (a) Fe(OH)₃ (50 nm), (c) Co(OH)₂ (50 nm), (e) Ni(OH)₂ (50 nm), (b) Fe(OH)₃ (500 nm), (d) Co(OH)₂ (500 nm), and (f) Ni(OH)₂ (500 nm) hollownanocubes under different scan rates. These data were used to present the plots showing the extraction of the CdI for different samples shown in Fig. 4(c) in the main text.

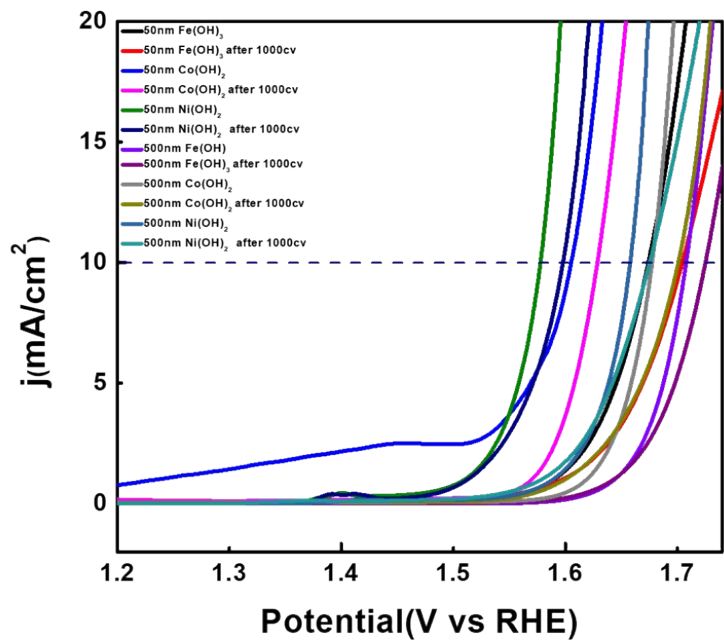


Fig. S14. Polarization curves of initial and 1000th cycles of all the catalysts.

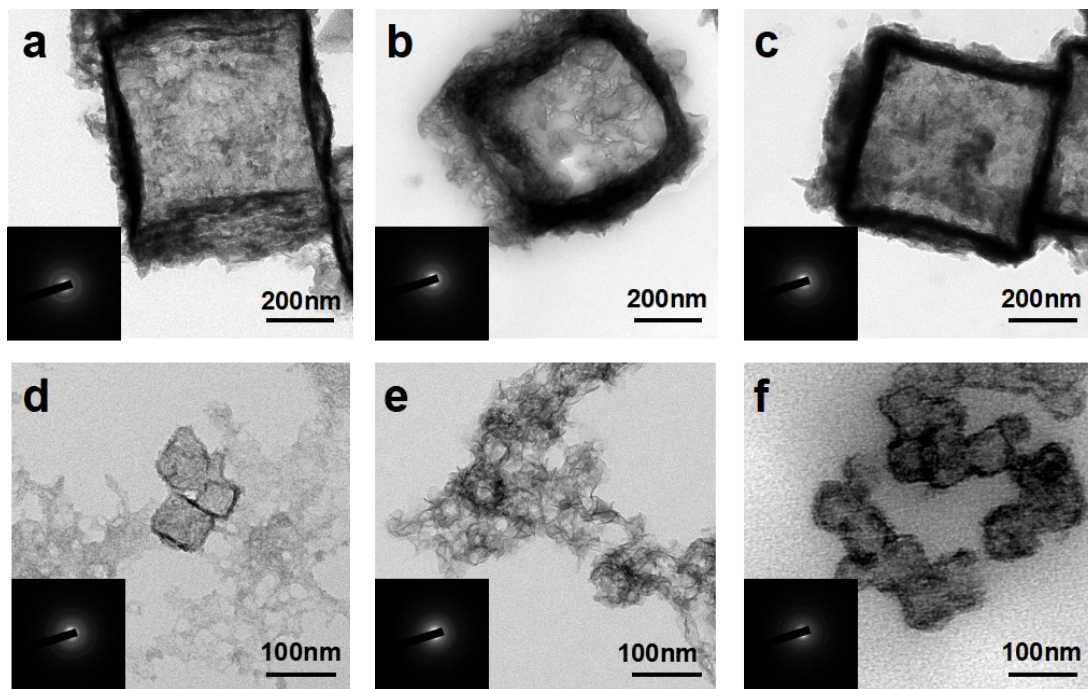


Fig. S15. TEM and SAED images of the as-prepared samples after 1000 CV cycles (a) Fe(OH)₃ (500 nm), (b) Co(OH)₂ (500 nm), (c) Ni(OH)₂ (500 nm), (d) Fe(OH)₃ (50 nm), (e) Co(OH)₂ (50 nm), (f) Ni(OH)₂ (50 nm) hollow nanocubes.

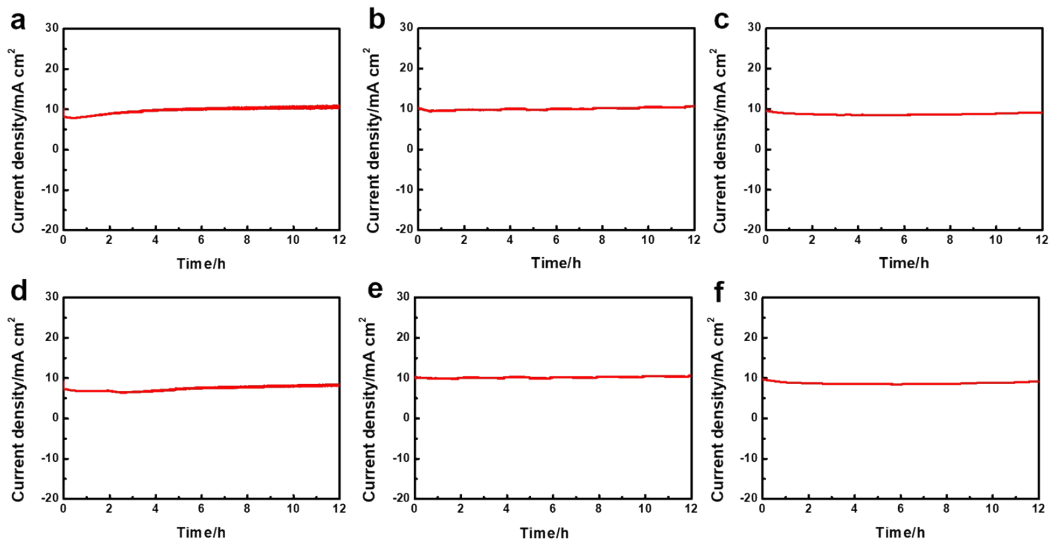


Fig. S16. $I-t$ curves of the as-prepared samples (a) $\text{Fe}(\text{OH})_3$ (500 nm), (b) $\text{Co}(\text{OH})_2$ (500 nm), (c) $\text{Ni}(\text{OH})_2$ (500 nm), (d) $\text{Fe}(\text{OH})_3$ (50 nm), (e) $\text{Co}(\text{OH})_2$ (50 nm), (f) $\text{Ni}(\text{OH})_2$ (50 nm) hollow nanocubes.

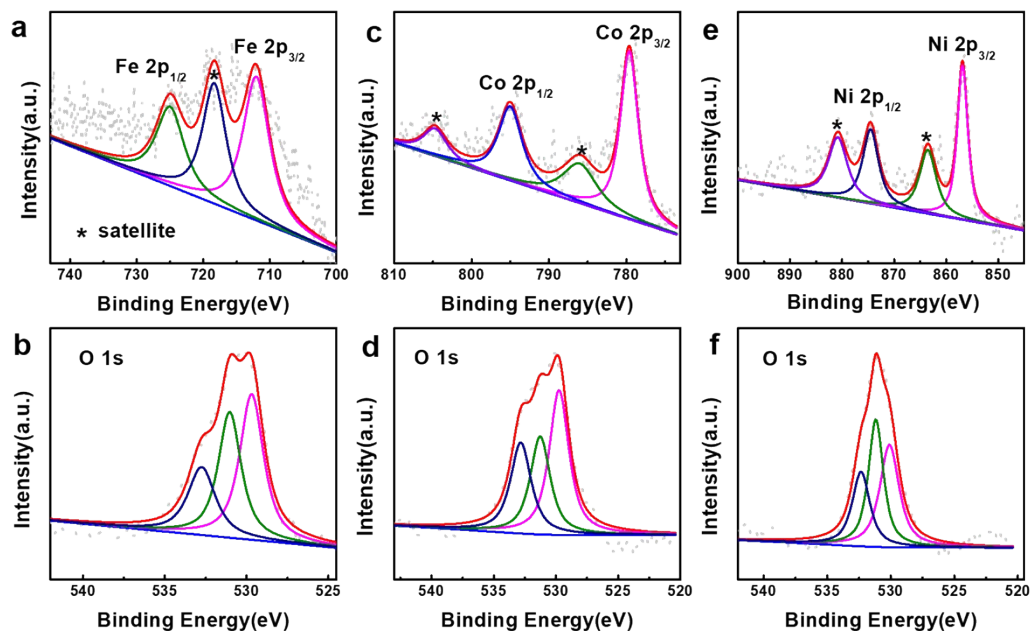


Fig. S17. XPS spectra of the as-prepared samples after the OER process: (a, b) iron hydroxide (500 nm), (c, d) cobalt hydroxide (500 nm), and (e, f) nickel hydroxide (500 nm).

Table S1. Comparison of Ni(OH)₂ (50 nm) hollow cubes with recently reported transition metal-based OER electrocatalysts.

Catalyst	η/mV (at 10 mA cm ⁻²)	Tafel slope (mV dec ⁻¹)	Ref
Ni(OH) ₂ hollow cubes	349	63	This work
CoO/Co composite	350	80	1
Ni/Ni ₃ C core/shell nanospheres	350	58	2
CoFe LDH nanosheets array	418	108	3
Au/NiFe LDH	237	-	4
Ni-β-FeOOH	247	44	5
NiFeS ultrathinnano sheets	312 (at 200 mA cm ⁻²)	-	6

References

1. X. Yuan, H. Ge, X. Wang, C. Dong, W. Dong, M. S. Riaz, Z. Xu, J. Zhang and F. Huang, *ACS Energy Lett.*, 2017, **2**, 1208-1213.
2. Q. Qin, J. Hao and W. Zheng, *ACS Appl. Mater. Inter.*, 2018, DOI: 10.1021/acsami.8b00716.
3. C. You, Y. Ji, Z. Liu, X. Xiong and X. Sun, *ACS Sustain. Chem. Eng.*, 2018, **6**, 1527-1531.
4. J. Zhang, J. Liu, L. Xi, Y. Yu, N. Chen, S. Sun, W. Wang, K. M. Lange and B. Zhang, *J. Am. Chem. Soc.*, 2018, **140**, 3876-3879.
5. Y. Liang, Y. Yu, Y. Huang, Y. Shi and B. Zhang, *J. Mater. Chem. A*, 2017, **5**, 13336-13340.
6. J. Zhang, Y. Hu, D. Liu, Y. Yu and B. Zhang, *Adv. Sci.*, 2017, **4**, 1600343